Article

Not peer-reviewed version

# Two-Phase Heat Transfer Devices in Thermal Control Systems of Electric Transport

Leonard Vasiliev *, Alexander Zhuravlyov *, Dmitry Sadchenko, Leonid Grakovich, Mikhail Rabetsky, Maksim Kuzmich, Alena Gasporovich

Posted Date: 5 May 2026

doi: 10.20944/preprints202605.0133.v1

Keywords: electric and hybrid vehicle; thermosyphon; double evaporator loop thermosyphon; passive thermal management; green technologies in transport

 doi:10.20944/preprints202605.0133.v1



*Article*

# Two-Phase Heat Transfer Devices in Thermal Control Systems of Electric Transport

**Leonard Vasiliev *, Alexander Zhuravlyov, Dmitry Sadchenko, Leonid Grakovich, Mikhail Rabetsky, Maksim Kuzmich and Alena Gasporovich**

Porous Media Laboratory, A.V. Luikov Heat and Mass Transfer Institute of the National Academy of Sciences of Belarus, Minsk 200072, Republic of Belarus

* Correspondence: leonard_vasiliev@rambler.ru

**Abstract**

The need to reduce harmful emissions and fossil fuel consumption has spurred the development of environmentally friendly technologies in the energy, industrial, and transportation sectors. One approach to addressing this problem is the active adoption of electric and hybrid powertrains in transportation, partially replacing internal combustion engines with them. With the development of electric transport, the growth of energy availability and the increase in mileage, the problem of ensuring optimal thermal conditions for the operation of engines, electronics, batteries and other equipment of electric vehicles is becoming increasingly important. This article examines methods for thermal management of electric vehicle equipment and the feasibility of using heat pipes and thermosyphons for these purposes. Based on the information obtained, the goal was to propose an effective, compact device for passive cooling of heat-loaded components in electric vehicles. The design and test results of an aluminum loop thermosyphon with two evaporators are presented. This loop thermosyphon is capable of simultaneously removing heat from two sources and transferring it to a single heat sink, thus replacing two thermosyphons and increasing the compactness of the thermal management system.

**Keywords:** electric and hybrid vehicle; thermosyphon; double evaporator loop thermosyphon; passive thermal management; green technologies in transport

## 1. Introduction

Air pollution has a negative impact on the environment, poses a health risk, and causes serious harm to living organisms. Greenhouse gas emissions in the transport sector are projected to increase by more than 20% by 2030 and by almost 50% by 2050 [1]. The largest contribution to air pollution comes from automobile transport. Figure 1 shows the distribution of greenhouse gas emissions by transport sector in the EU as of 2022 [2].

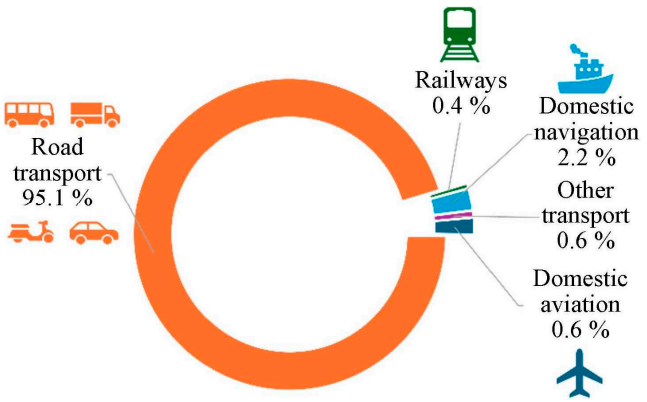


**Figure 1.** Greenhouse gas emissions from different modes of transport in the EU as of 2022 [2].

 doi:10.20944/preprints202605.0133.v1



To improve environmental safety, it is necessary to take measures to reduce the amount of emissions of anthropogenic pollutants. The intensive development of hybrid and electric technologies in automobile, urban passenger (electric buses, autonomous trams), aviation and water transport makes it possible to solve the problems of reducing the consumption of hydrocarbon fuels and improving the environmental situation. The positive qualities of electric transport include simplicity and reliability, as well as lower maintenance costs and required electricity compared to traditional vehicles. A comparison of the energy cost per kilometer for electric vehicles (EVs) and internal combustion engine (ICE) vehicles is shown in Figure 2 [3]. Due to these advantages, and despite the fact that EVs have inferior range to their ICE counterparts and the fact that charging the battery can take several hours, EVs are becoming increasingly widespread.

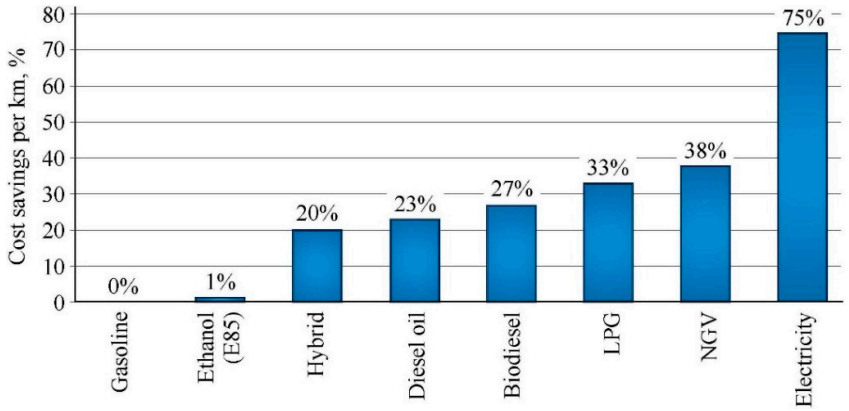


**Figure 2.** Comparison of cost savings per kilometer achieved by vehicles running on different fuel types [3].

Converting a portion of the aircraft fleet to electric power will have a positive impact on environmental improvement. Given the significant progress in the development of electrical system components, various aircraft concepts with electric and hybrid (turboelectric) propulsion systems (PS), including those using components based on high-temperature superconductivity, are being considered. Currently, the greatest practical impact lies in the development of medium-sized hybrid aircraft. Small hybrid aircraft have already been put into practice, while large ones, according to the authors [4], are still the subject of conceptual analysis, a situation that will persist for the foreseeable future until the evolution of energy storage technologies yields the desired results. The characteristics of the electronic equipment of an electric aircraft include high heat generation intensity, large distances between heat sources and sinks, and dense arrangement of components.

Electric jet skis, ferries, and electric boats are now widely used on rivers and seas. Given the cost and power of currently available batteries, electric propulsion makes sense for smaller pleasure craft that don't require high-power engines or a long range. The quiet operation of the engine and the absence of unpleasant exhaust odors make boating more comfortable. Large-capacity vessels utilize a technology that transfers electrical energy from a heat engine to a propulsion motor. This system includes power generation, coordination, and conversion of its parameters to control the propulsion motor. The transition to electric propulsion will enable watercraft to comply with evolving environmental standards.

Vehicles with electric and hybrid powertrains contain heat-loaded components that require thermal management. Heat sources include the rotor and stator of the electric motor, power electronics equipment—switching devices (converters/inverters, high-current chips, switches, bipolar transistors), navigation electronics, on-board chargers, headlights, etc. (Figures 3 [5], 4 [6], 5 [7], and 6 [8]). The performance and safety of this equipment depends on the effective management of its thermal operating conditions, so it requires optimal thermal regulation.

 doi:10.20944/preprints202605.0133.v1



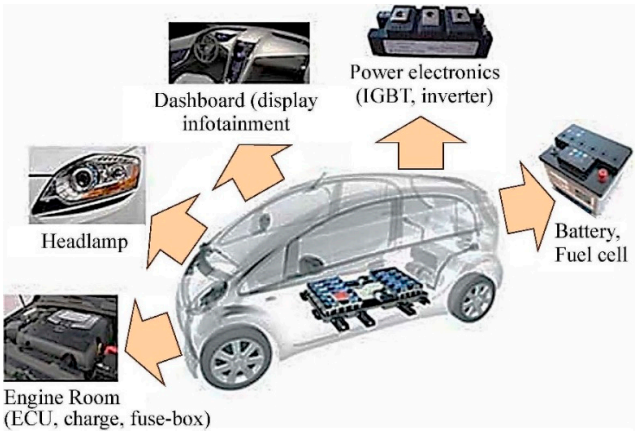


**Figure 3.** Thermally loaded components of an electric vehicle [5].

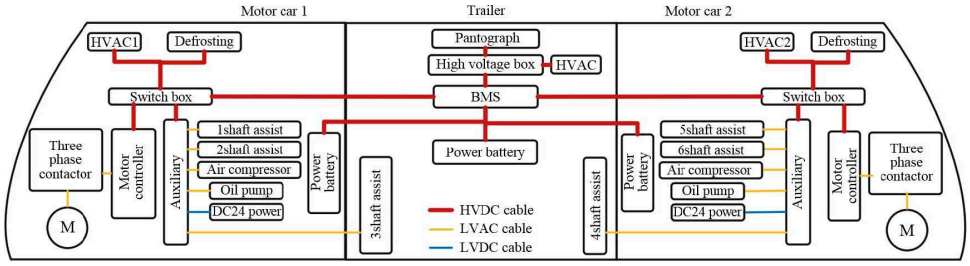


**Figure 4.** Traction and auxiliary power system of a rapid autonomous tram [6].


**Figure 5.** Thermal management system (TMS) of an aircraft with a hybrid power plant [7].

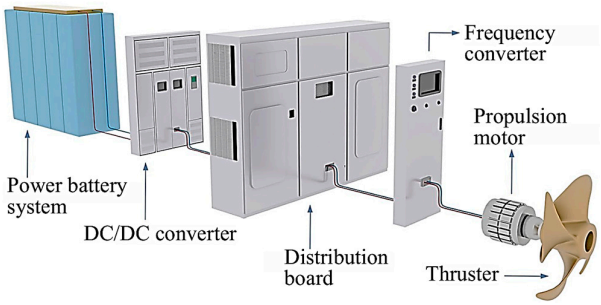


**Figure 6.** Thermally loaded objects of the ship's electric propulsion system [8].

 doi:10.20944/preprints202605.0133.v1



Thermal management is key to ensuring such important characteristics of electric vehicles as energy efficiency and range, reliability, service life, safety, and crew and passenger comfort. The relationship between thermal management and the main characteristics of an electric vehicle is illustrated in Figure 7 [2].

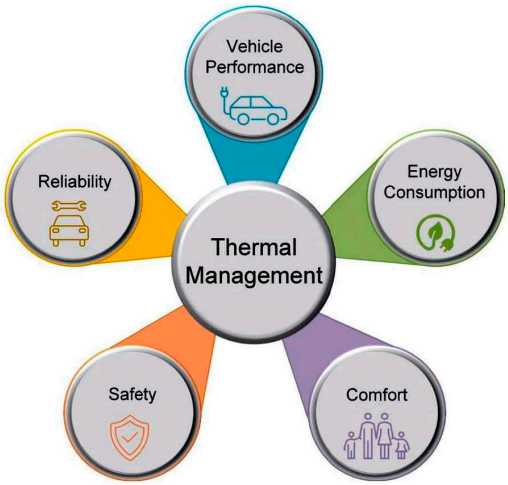


**Figure 7.** Relationship of thermal management with the main characteristics of an electric vehicle [2].

The successful operation of electric vehicles is determined by the reliable operation of the engine and the appropriate choice of power sources. Electricity is generated by the battery through a chemical reaction, accompanied by heat generation caused by internal ohmic resistance and entropy changes resulting from electrochemical reactions [9]:

$$\dot{q} = R_i i^2 - T\Delta S \frac{i}{F}, \qquad (1)$$

where $\dot{q}$ is the rate of internal heat release per unit volume, $R_i$ is the internal equivalent resistance, $i$ is the discharge rate per unit volume, $\Delta S$ is the entropy change, and $F$ is the Faraday constant. Different types of lithium-ion batteries have different values of internal resistance and entropy change. Internal resistance depends on both the temperature and the battery's state of charge.

Batteries must have sufficient specific power and energy, a long service life, and avoid self-discharge while parked. Lithium-ion batteries are the most promising. They offer higher specific energy than other energy storage technologies, high voltage, a fast charging process, low self-discharge, and a long service life. However, these energy storage devices are susceptible to both overcooling and overheating, and they are also sensitive to temperature differences between individual cells. Extremely high and low temperatures significantly reduce battery performance and longevity (Figure 5). The optimal operating temperature range for these batteries is from -25°C to 40°C, with the temperature difference between cells not exceeding 5°C. Low temperatures reduce their capacity and lead to self-discharge. Excessive or uneven temperature increases in a module or unit increase the risk of fire and explosion and significantly reduce their service life. Therefore, the design of an electric vehicle's power plant must include a system for effective heat dissipation and protection of energy storage devices from thermal runaway, which can lead to fire or even explosion due to electrolyte breakdown at temperatures above 150 °C. For operation of lithium-ion and other batteries, a safe and reliable operating area, i.e. temperature and voltage window, must be provided, Figure 8 [10].

 doi:10.20944/preprints202605.0133.v1



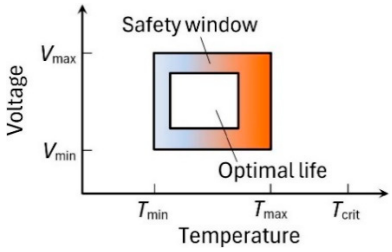


**Figure 8.** Lithium-ion battery cell safety window [10].

Various systems can be used for thermal control of heat-generating objects in electric transport: air, liquid, using phase-change materials, thermoelectric, immersion in boiling liquid, including in combination with heat pipes [11–20]. The classification of cooling systems is shown in Figure 9 [17]. A free-convection air system is simple, relatively inexpensive, and electrically safe. However, due to the low heat capacity and thermal conductivity of air, it is effective only when intensive airflow over the radiators is possible. Liquid cooling is more efficient, but requires a coolant reservoir and an energy-consuming pumping system. Phase-change materials maintain a constant temperature of the object and are energy-efficient, but they allow for molten material leakage and are limited in the available latent heat. Thermoelectric coolers based on the Peltier effect are capable of precisely controlling the object's temperature, are reliable, silent, compact, lightweight, and easy to operate, but are less efficient than other systems.

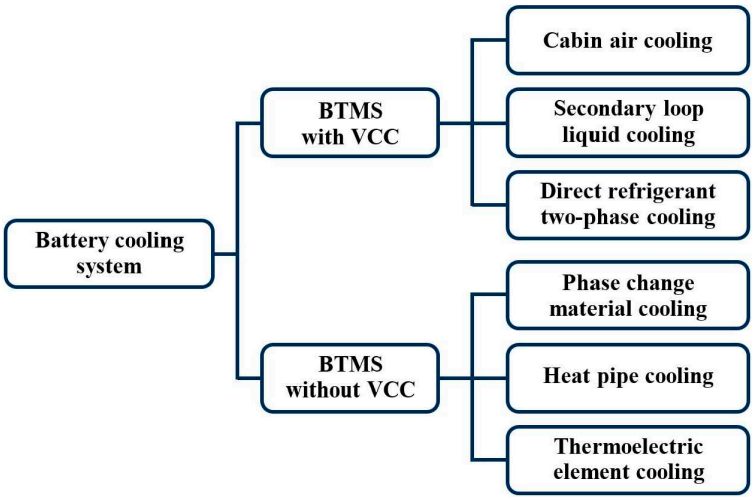


**Figure 9.** Classification of batteries thermal management systems. VCC is the vapor compression cycle [17].

In electric vehicles, the dissipated heat is absorbed by the surrounding air. The same approaches used in electric vehicles can be used to ensure thermal control of electric watercraft. In electric aircraft, the heat sinks are the oncoming airflow and the aircraft structure, which is also cooled by air. Effective intermediate links between heat sources and heat sinks are heat pipes (HP) and two-phase thermosyphons (TS) – autonomous closed devices with a higher effective thermal conductivity than metals, including copper and silver. The use of passive systems eliminates the need for coolant pumps and local blower fans, resulting in savings on the electricity required to power electric motors.

An evaporation-condensation cycle occurs within the HP and the TS, both filled with liquid. In the evaporator, heat from an external source causes evaporation. The vapor moves to the condenser, where it condenses, releasing heat that can be put to good use. In the HP, the liquid phase returns from the condenser to the evaporator under the action of capillary pressure in the microchannels of a porous wick (Figure 10). A thermosyphon is a heat pipe in which condensate flows into the evaporator under the force of gravity. Therefore, a TS works only if the evaporator is located below

 doi:10.20944/preprints202605.0133.v1



the condenser. This condition is not required for a HP. However, the design of thermosyphons is simpler than that of heat pipes, and they are cheaper due to the absence of a wick structure. Heat pipes and thermosyphons are easy to operate, have no moving parts, require no energy or maintenance, and can provide virtually lossless heat exchange between the surface of the cooled object and the external environment. They can be used to effectively remove heat from heat-loaded objects.

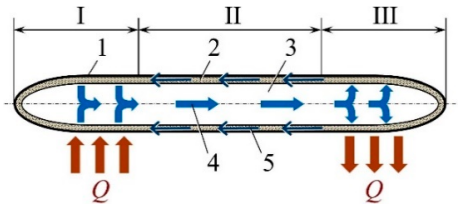


**Figure 10.** Heat pipe: I) evaporator, II) adiabatic zone, III) condenser, 1) case, 2) capillary wick, 3) vapor channel, 4) vapor flow, 5) liquid flow, *Q* is a heat flow.

In electric transport, as in transport in general, minimizing the weight and size of components and systems is crucial. The purpose of this study was to examine various thermal management methods for electric vehicle equipment and propose an effective, compact device for passive cooling of heat-loaded components in electric vehicles. This article presents the results of a study of an aluminum loop thermosyphon equipped with two evaporators. The device is capable of simultaneously removing heat from two sources and transferring it to a single heat sink, thus replacing two thermosyphons and increasing the compactness of the thermal control system.

## 2. Loop Thermosyphons in Thermal Management Systems

Loop thermosyphons (LTS) are becoming widely used. The difference between a LTS and a conventional TS is the separate flow of vapor and liquid through separate channels for each phase of the coolant. The coolant returns from the condenser to the evaporator through the liquid pipe under the force of gravity, while the vapor from the evaporator is transferred to the condenser through the vapor pipe under the pressure differential between the evaporator and condenser, caused by the temperature difference in these zones. The absence of friction between the steam and liquid flows increases the heat transfer capacity of the LTS compared to conventional TS. Figure 11 shows a diagram of a LTS with a horizontal evaporator and condenser [21].

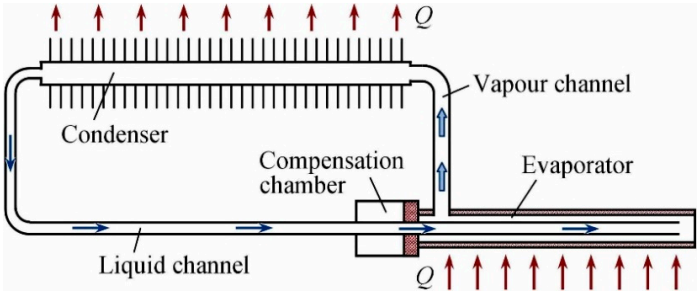


**Figure 11.** Loop thermosyphon with a cylindrical horizontal evaporator and an air-cooled radiator in the condenser.

Loop thermosyphons offer greater installation flexibility than TS. The evaporator and condenser of a loop thermosyphon can be positioned horizontally. The presence of tubes for vapor and liquid flows allows heat flow from the cooled object to a remote heat sink. This type of thermosyphon is

 doi:10.20944/preprints202605.0133.v1



used to cool various heat-sensitive equipment, including in electric vehicles. Figure 12 [22] shows an example of a loop thermosyphon being used in a power electronics temperature control system.

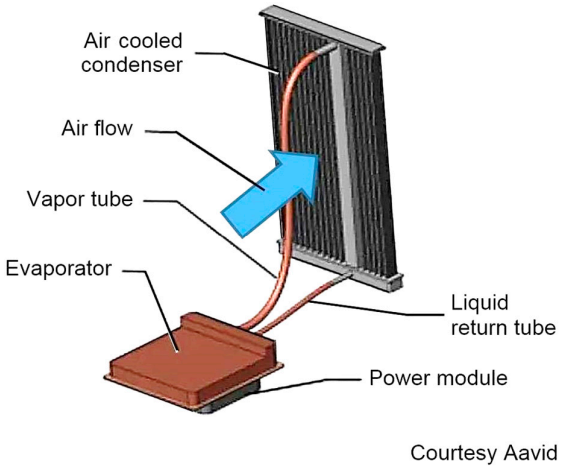


**Figure 12.** Loop thermosyphon with air-cooled radiator for thermal control of the power module [22].

The authors of the study [23] experimentally investigated the use of a LTS in a potential thermal control system in railway traction motors as an alternative to a traditional forced-air cooling system (Figure 13). The LTS system demonstrated suitable performance in normal operation under overload conditions of up to 560 W.

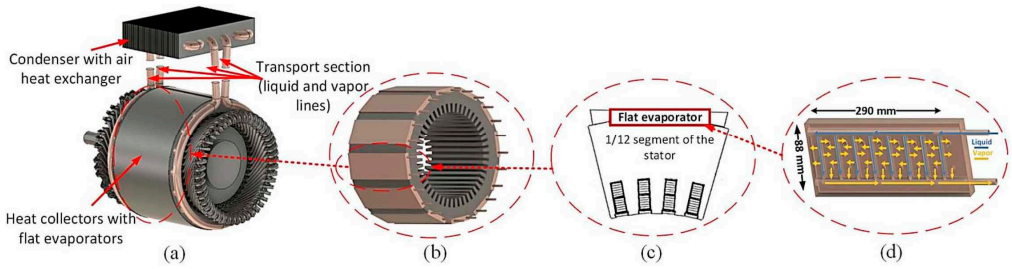


**Figure 13.** Cooling system of an electric motor with a LTS: (a) general view, (b) flat LTS evaporators on the stator of the electric motor, (c) stator segment in combination with a flat LTS evaporator, (d) internal structure of the LTS evaporator [23].

## 3. Materials and Methods

*3.1. Aluminum Thermosyphon with Two Evaporators and One Condenser*

The Luikov Heat and Mass Transfer Institute of the National Academy of Sciences of Belarus has accumulated extensive experience in the development and research of heat transfer systems and heat exchangers, including those applicable to electric transport [21,24,25]. Considering the need to reduce the weight of vehicle equipment, an aluminum loop thermosyphon with two multi-channel evaporators and one condenser was developed (Figure 14). The evaporators are flat for easy mounting of the cooled components on their surface. The tight fit of the temperature-controlled components to the evaporator minimizes thermal contact resistance. Since wetting a large vertical surface is difficult, the evaporator's interior is divided into parallel channels, improving the supply of liquid to the zones of vapor generation. The evaporator is made of ALS-7PK70_011.1 extruded profile. Curved meniscus formed on the channel walls generates the capillary pressure necessary for the liquid phase to spread along the channel's height. Dividing the evaporator's interior into channels also helps regulate the flow and laminarize the resulting vapor, which is discharged through the

 doi:10.20944/preprints202605.0133.v1



vapor manifold and vapor tube into the condenser. The liquid tube (condensate line) runs along the liquid collector along its entire length (Figure 15), the condensate flows into the gap between the tube and the collector body, changes direction to the opposite, fills the gap and, moving along the formed slot channel, supplies the evaporator 1 with the liquid phase, then the evaporator 2.

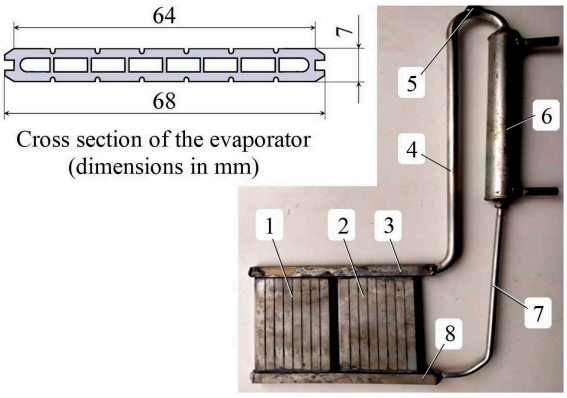


**Figure 14.** Aluminum loop thermosyphon with two evaporators: 1, 2) evaporators; 3, 8) vapor and liquid collectors; 4) vapor tube; 5) filling nozzle; 6) condenser; 7) liquid tube.

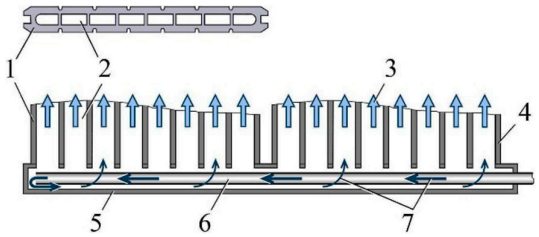


**Figure 15.** The end section of the condensate line in the liquid collector: 1) evaporator 1, 2) evaporator channel, 3) flow of generated vapor, 4) evaporator 2, 5) liquid collector, 6) liquid tube (condensate line), 7) condensate flow.

### *3.2. Experimental Equipment and Experimental Procedure*

#### 3.3.1. Experimental Setup

The experiments were carried out on a setup equipped with thermosyphon mounting units, systems for supplying heat to evaporators and cooling the condenser, and a data processing unit (Figure 16).

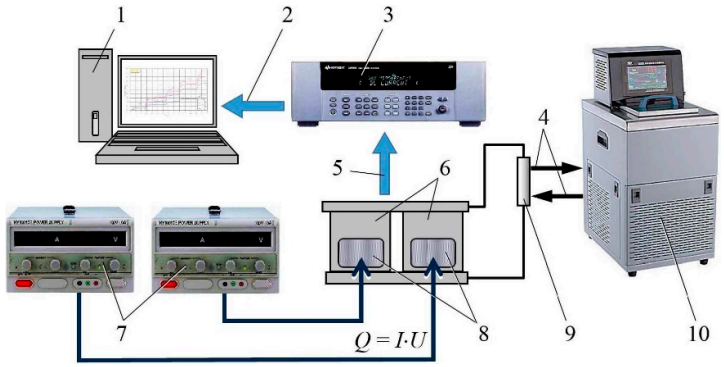


**Figure 16.** Experimental setup diagram: 1) personal computer, 2) experimental data, 3) Agilent Data Loger multimeter, 4) coolant, 5) signals from thermocouples, 6) thermosyphon evaporators, 7) pulse power supplies, 8) heaters, 9) thermosyphon condenser, 10) cryothermostat.

 doi:10.20944/preprints202605.0133.v1



The heat flow to the evaporator was supplied by an ohmic heater powered by a Mastech HY10010E DC power source with a voltage setting accuracy of 1 V and a current of 0.1 A. Heat was removed from the condenser by a flow-through liquid heat exchanger of the "pipe in pipe" type, the temperature of the coolant in the heat exchanger was stabilized by an LOIP FT-316-40 cryothermostat with a temperature maintenance accuracy of ±0.1 °C. T-type (copper-constantan) thermocouples were installed at the temperature measurement points. The signals from the thermocouples were processed by an Agilent 34980A multimeter and transmitted to a computer for data analysis. To minimize heat transfer to the external environment, the thermosyphon components were insulated.

3.3.2. Experimental Procedure

During the study of the KTS, temperatures were measured on the surface of the thermosyphon, and heat transfer coefficients on the vapor generation surfaces of the evaporators were determined.. Acetone was used as the working fluid, taking into account the chemical compatibility of these materials [26]. Before the experiments, the thermosyphons were leak-tested with an excess air pressure of 0.3 bar for 24 hours.

The experimental methodology involved a stepwise change in the value of the supplied heat flow, either increasing or decreasing, in accordance with the experimental program, and a holding period between changes in the heat load for a certain period of time, during which the thermal parameters of the thermosyphon, which have undergone changes, stabilize, and a steady-state mode of its operation is established. The heat flux supplied to the evaporators was estimated based on the electrical power level of the *I*×*U* heaters, taking into account heat losses in the wires and leaks through the thermal insulation. Heat losses by radiation to the environment were determined as

$$Q_{rad} = \varepsilon\sigma A_{rad}\left(\bar{T}_{srf}^4 - T_{amb}^4\right), \qquad (2)$$

where $\varepsilon$ = 0.77 is the degree of surface blackness; σ = 5.67×10$^{-8}$ W m$^{-2}$ K$^{-4}$ is the Stefan-Boltzmann constant; $A_{rad}$ is the area of the radiating surface, m$^2$; $\bar{T}_{srf}$ is the average temperature of the outer surface of the thermal insulation; $T_{amb}$ is the ambient temperature (room temperature).

Temperature measurement uncertainness were calculated using the formula

$$U_{\text{total}} = \sqrt{U_{\text{instr}}^2 + U_{\text{FJC}}^2 + U_{\text{rand}}^2}, \qquad (3)$$

Here:

$U_{\text{instr}}$ is the uncertainty of the device, depending on the resolution of the data recorder and the accuracy of voltage measurement (specified in the device documentation);

$U_{\text{RJC}}$ is the cold junction compensation (automatically measured terminal temperatures in the data logger);

$U_{\text{rand}}$ is the uncertainty of random fluctuations; it is much smaller than the instrument error and the cold junction compensation error and can be neglected.

Calculations showed that the measurement uncertainties did not exceed 6.6 %.

## 4. Results and Discussion

*4.1. Study of a Two-Evaporator Aluminum Thermosyphon*

The ability of a loop thermosyphon with two evaporators to remove heat from two heat-loaded objects with the same or different levels of heat generation was experimentally tested. The heat transfer characteristics of the thermosyphon were determined using the following heat load application schemes:

– evaporator 1 is loaded while evaporator 2 is unloaded;

– both evaporators are loaded.

 doi:10.20944/preprints202605.0133.v1



4.1.1. Operation of a Two-Evaporator Thermosyphon with One Evaporator Heat Loaded

In the first stage, the heat load on the evaporator was applied to evaporator 1 and increased from 40 to 80 W in 20-W increments. Experiments with varying amounts of charged fluid showed that for this heat load configuration, within the studied range of transferred heat fluxes, the optimal fill factor $\psi = V_{wf}/V_e$ ($V_{wf}$ is working fluid volume) is 30–70%, at which the intensity of heat exchange during vaporization on the evaporator walls is highest. The surface temperature values of the thermosyphon components are shown in Figure 17. The location of the thermocouples is shown in Figure 18.

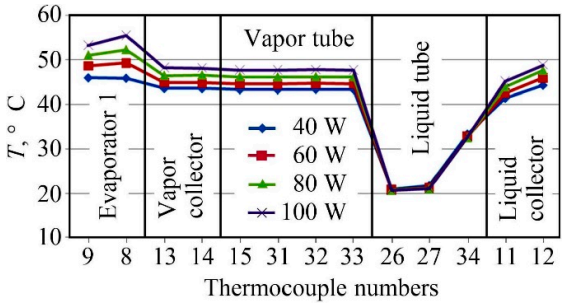


**Figure 17.** Temperature distribution over the surface of a thermosyphon ($\psi$ = 40 %).

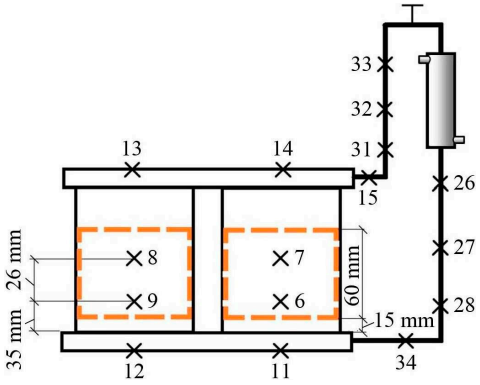


**Figure 18.** Thermocouple arrangement diagram on a thermosyphon.

At heat fluxes of 40 and 60 W, the heat-loaded evaporator 1 is practically isothermal. As the heat load increases, the temperature at the top of the evaporator (thermocouple 8) rises because the liquid level in the vertical channels of the evaporator decreases. This decrease occurs because the intensity of the vaporization process increases, and the condenser at $\psi$ = 40% loses its ability to supply the evaporator with liquid sufficient to wet the entire heating surface. However, the thermosyphon continues to function reliably, and a 40% filling level, as with a single evaporator, ensures this stability. An increase in temperature with increasing heat load in the upper part of a vertically positioned evaporator has also been noted in studies [27,28], the authors of which also attribute this phenomenon to localized dehydration of the heat exchange surface.

4.1.2. Operation of a Two-Evaporator Thermosyphon with a Heat Load on Two Evaporators

Figure 19 shows a graph of the temperature field evolution on the surface of a loop thermosyphon over time when it was filled with 33% working fluid (acetone). The heat flow ($Q$ = 40 W) was supplied to evaporator 1; evaporator 2 functioned as an auxiliary condenser and accelerated the start-up of the thermosyphon. During the transition phase (section I on the τ axis), transient heating of evaporator 1 occurs. Vapor does not enter the thermosyphon vapor tube until the saturation temperature in the vapor manifold reaches 60°C. After the temperature of evaporator 2

 doi:10.20944/preprints202605.0133.v1



rises to the saturation temperature during the condensation of vapor from evaporator 1, the operation of the LTS condenser is activated and a steady-state heat transfer process is established (stage II).

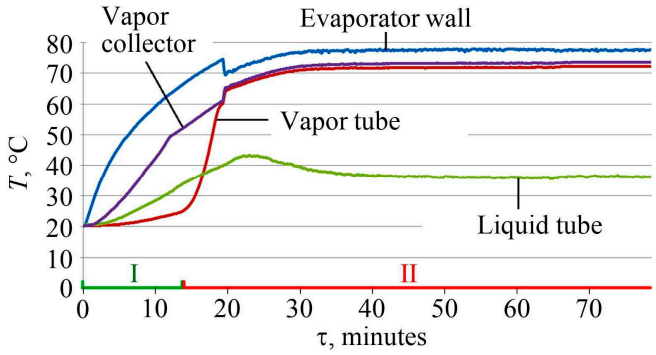


**Figure 19.** Starting a two-evaporator condensing unit with a load on evaporator 1. Working fluid is acetone (ψ = 33%), $Q$ = 40 W.

Next, the optimal amount of working fluid was determined for efficient operation of the device when both evaporators are under load. In this case, the processes in evaporators 1 and 2 interact with each other, ultimately affecting the operation of the entire device. The amount of working fluid in the thermosyphon loop Optimization is complicated by the fact that the evaporators may operate with unequal heat flows. It was experimentally established that when both evaporators are turned on in the current range of thermal loads of 40–100 W for each evaporator, effective heat transfer by the thermosiphon is ensured at a filling ratio of 60%.

The operation of a loop thermosyphon with two evaporators under asymmetric heat loads was studied. At constant heat loads of 40 W, 60 W, and 80 W on evaporator 1, different heat flows were supplied to evaporator 2 (Figure 20).

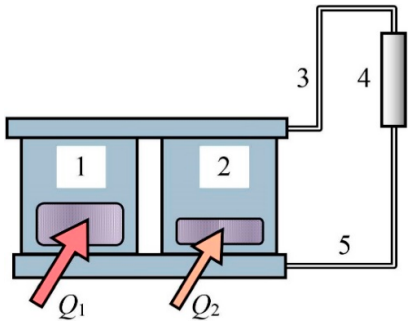


**Figure 20.** Asymmetric load on a condensing unit with two evaporators: 1, 2) evaporators 1 and 2; 3) vapor line; 4) condenser; 5) condensate line; $Q_1$, $Q_2$ are heat loads on evaporators 1 and 2.

Experiments have shown that the operation of evaporator 2 has little effect on the thermal characteristics of evaporator 1. Figures 21a and 21 b show data obtained at heat load values of 40 W and 80 W on evaporator 1. The heat transfer coefficients were determined as

$$h_i = \frac{Q_i}{A_i\left(\bar{T}_{e,i} - \bar{T}_{v,i}\right)}, \qquad (4)$$

where $A_i$ is the contact area of evaporator 1 or 2 and heaters.

 doi:10.20944/preprints202605.0133.v1



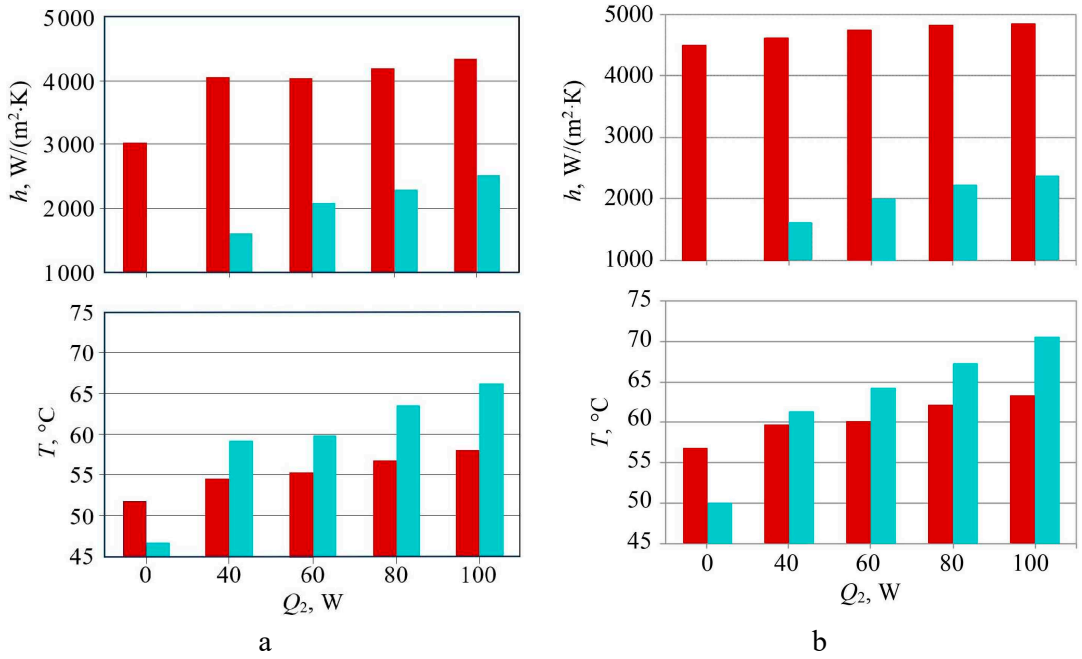


**Figure 21.** Heat characteristics of evaporators 1 and 2 at heat loads $Q_1$ = 40 W (a) and $Q_1$ = 80 W (b) per evaporator 1 (■) and variable load $Q_2$ on evaporator 2 (■).

It has been established that increasing the heat load on one evaporator while maintaining a constant load on the second evaporator has virtually no effect on the intensity of heat exchange in the second evaporator and is accompanied by a minor (no more than 3 °C) increase in its surface temperature. This circumstance must be taken into account when designing thermal control systems for onboard equipment in electric vehicles. Nevertheless, the results of the study indicate that the two-evaporator thermosyphon of the presented design is capable of simultaneously cooling several objects with different levels of heat generation, while the negative impact of evaporator 2 on the thermal properties of evaporator 1 is minimal.

## 5. Conclusions

The rapid development of hybrid and electric technologies in automobile, aviation, and water transport is helping to reduce fossil fuel consumption and improve environmental conditions. As the energy requirements of vehicles increase, the challenges of ensuring optimal thermal performance for engines, electronics, batteries, and other equipment are becoming more pressing. Heat pipes and thermosyphons can be used to effectively remove heat from heat-stressed objects.

The relevance of the conducted research is associated with the growth in the power of electronic and electrical equipment, accompanied by increased heat generation, and the resulting need for new cooling systems that are capable of removing high-density heat flows from heat-stressed electronic elements.

The following results were obtained:

1. A series of tests was conducted on an aluminum loop thermosyphon with two flat multi-channel evaporators connected by common manifolds for transporting vapor and working fluid. The use of aluminum as a structural material provides significant weight savings, which is crucial for transport, especially aviation. The thermosyphon's flat evaporator maintains good thermal contact with the objects being cooled. Consequently, not just one, but several cooled elements can be connected to a thermosyphon evaporator consisting of several multi-channel evaporators.
2. When designing thermal control systems for on-board equipment of electric transport, it should be borne in mind that an increase in the thermal load on one evaporator with a constant load on

 doi:10.20944/preprints202605.0133.v1



the second evaporator is accompanied by an insignificant (no more than 3 C) increase in the temperature of its surface.

3. The created device can be recommended for use in passive cooling systems for powerful electronic components of electric and hybrid transport, avionics, telecommunications equipment, laser technology, and other heat-loaded objects.

Future research should focus on modifying the heat-exchange surfaces of thermosyphon evaporators to increase the intensity of heat transfer during vapor generation. A successful solution to this problem will enable the improvement of the heat transfer capacity of the two-phase loop thermosyphon and the miniaturization of the device.

## References


1. Kovačević, T.; Kljajić, R.; Glavaš, H.; Kljajin, M. Analysis of the impact of electromobility on the distribution grid. *World Electr. Veh. J.* **2025**, *16(7)*, 358, https://doi.org/10.3390/wevj16070358
2. Martin, G.E.; Baghdadi, M.E.; Hegazy, O. Advancements in thermal management for electric vehicles: Strategies, architectures, and power electronics cooling. *IEEEAccess* **2025**, *13*, 147511–147544.
3. Sanguesa, J.A.; Torres-Sanz, V.; Garrido, P.; Martinez, F.J.; Marquez-Barja, J.M. A Review on electric vehicles: technologies and challenges. *Smart Cities* **2021**, *4*, 372–404, https://doi.org/10.3390/smartcities4010022
4. Xie Y.; Savvarisal, A.; Tsourdos, A.; Tsourdos, A.; Zhang, D.; Gu, J. Review of hybrid electric powered aircraft, its conceptual design and energy management methodologies. *Chinese J. of Aeronautics* **2021**, *34(4)*, 432–450, https://doi.org/10.1016/j.cja.2020.07.017.
5. Singh, R.; Mochizuki, M.; Saito, Y.; Yamada, T.; Thang Nguyen; Tien Nguyen. Heat pipe applications in cooling automotive electronics. *Heat Pipe Sci. and Technol.: An Intern. J.* **2016**, *7(1–2)*, 57–69.
6. Jianghua Feng, Yunqing Hu, Xiwen Yuan, Ruipeng Huang, Lei Xiao, Chenlin Zhang. Autonomous-rail rapid transit tram: System architecture, design and applications. *Green Energy and Intelligent Transportation* **2024**, *3*, 100161, https://doi.org/10.1016/j.geits.2024.100161.
7. Affonso, W, Jr.; Gandolfi, R.; Nunes dos Reis, R.J.; Ilário da Silva, C.R.; Rodio, N.; Kipouros, T.; Laskaridis, P.; Chekin, A.; Ravikovich, Y.; Ivanov, N.; Ponyaev, L.; Holobtsev, D. Thermal management challenges for HEA – FUTPRINT 50. *IOP Conf. Series: Mater. Sci. Engin.* **2021**, 1024, 012075 – DOI: 10.1088/1757-899X/1024/1/012075.
8. Jia, F.; Lee, G. Simulation of battery thermal management system for large maritime electric ship's battery pack. *Energies* **2024**, *17*, 4587, https://doi.org/10.3390/en17184587.
9. Karimi, G.; Dehghan, A.R. Thermal management analysis of a lithium-ion battery pack using flow network approach. *Int. J. Energy Res.* **2014**, *38*, 1793–1811. https://doi.org/10.1002/er.3173.
10. Bisschop, R.; Willstrand, O.; Amon, F.; Rosengren, M. *Fire Safety of Lithium-Ion Batteries in Road Vehicles*. RISE Report 2019:50, RISE Research Institutes of Sweden AB. Borås, 2019. 105 p.
11. Gómez Díaz, K.Y.; De León Aldaco, S.E.; Aguayo Alquicira, J.; Ponce Silva, M.; Portillo Contreras, S.; Sánchez Vargas, O. Thermal Management Systems for Lithium-Ion Batteries for Electric Vehicles: A Review. *World Electr. Veh. J.* **2025**, 16, 346. https://doi.org/10.3390/wevj16070346.
12. Sharifi, N.; Shabgard, H.; Millard, C.; Etufugh, U. Hybrid heat pipe-PCM-assisted thermal management for lithium-ion batteries. *Batteries* **2025**, *11*, 64, 96–120, https://doi.org/10.3390/batteries11020064.
13. Zhang, S.; Zheng, X.; Chen, D.; Huang, Y.; Yuan, W.; Tang, Y.; G. Chen. Thermal management of lithium-ion battery integrated with ultra-thin vapor chamber. *Energy Convers. and Manag.* **2025**, *345*, 120417. https://doi.org/10.1016/j.enconman.2025.120417.
14. Zhou, H.; Dai, C.; Liu, Y.; Fu, X.; Du, Y. Experimental investigation of battery thermal management and safety with heat pipe and immersion phase change liquid. *J. of Power Sources* **2020**, *473*, 228545, https://doi.org/10.1016/j.powsowr.2020.228545.
15. Ye, X.; Zhao, Y.; Quan, Z. Experimental study on heat dissipation for lithium-ion battery based on micro heat pipe array (MHPA). *Appl. Therm. Eng.* **2018**, *130*, 74–82, https://doi.org/10.1016/j.applthermaleng.2017.10.141.

 doi:10.20944/preprints202605.0133.v1



16. Singh, R.; Lapp, G.; Velardo, J.; Long, P.T.; Mochizuki, M.; Akbarzadeh, A.; Date, A.; Mausolf, K.; Busse, K. Battery cooling options in electric vehicles with heat pipes. *Frontiers in Heat and Mass Transf. (FHMT)* **2021**, *16(2)*, 1–8, https://doi.org/10.5098/hmt.16.2.
17. Kim, J.; Oh, J.; Lee, H. Review on battery thermal management system for electric vehicles. *Appl. Therm. Eng.* **2019**, *149*, 192–212. https://doi.org/10.1016/j.applthermaleng.2018.12.020.
18. Li, Y.; Bian, X.; Li, H.; Yu, H.; Tao, H. Thermal management of electric bus batteries simulation study using heat pipes and phase change materials under varying passenger capacity and actual driving routes. *Appl. Therm. Eng.* **2025**, *273*, 126402. https://doi.org/10.1016/j.applthermaleng.2025.126402.
19. Miś, P.; Miś, K.; Waszczuk-Młyńska, A. The impact of the cooling system on the thermal vanagement of an electric bus battery. *Appl. Sci.*. **2025**, *15*, 9776. https://doi.org/10.3390/app15179776.
20. Yadav, P.; Jinadasa, L.; Wray, A.; Petrovich, S.; Georgiou, M.; Ebrahim, K. Battery electric vehicle thermal management system modelling and validation. *Thermo*, **2026**, *6*, 4. https://doi.org/10.3390/thermo6010004.
21. Vasiliev, L.L.; Zhuravlyov, A.S. Two-phase heat transfer devices for passive cooling of electric and hybrid aircraft onboard equipment. *Int. J. of Sustainable Aviation* **2023**, *9(2)*, 89–114, https://doi.org/10.1504/IJSA.2023.129938.
22. Kang, S.S. Advanced Cooling for Power Electronics. *Electronic Thermal Engineering SEMI-THERM 2026*, San Jose, California (CA), March 9–12, 2026.
23. Ghahfarokhi, P.S.; Rasilo, P.; Cardoso, A.J.M.; Ušakovs, I.; Mishkinis, D.; Podgornovs, A. Proof of concept of a two-phase thermal management system for railway traction motors. *IEEE Transactions on Energy Conversion* **2026**, *41(1)*, 19–28, https://doi.org/10.1109/TEC.2025.3583076.
24. Vasiliev, L.L.; Zhuravlyov, A.S.; Kuz'mich, M.A. Experimental study of hydrodynamics and heat transfer in a loop thermosyphon for thermal control of power plants of electric aircraft. *Therm. Eng.* **2025**, *6*, 499–504. – https://doi.org/10.1134/S0040601525700168.
25. Vasiliev, L.; Zhuravlyov, A.; Sadchenko, D. Two-phase heat conductors for passive thermal regulation systems of electric vehicles. *Mechanical Engineering Advances* **2025**, *3(2)*, 2052, https://doi.org/10.59400/mea2052.
26. Reay, D.; Kew, P. *Heat Pipes*. Fifth Edition. Butterworth-Heinemann is an imprint of Elsevier, Linacre House, Jordan Hill, Oxford OX2 8DP, 2006; 377 p.
27. Zhang, T.; Qu, J.; Hua, Y. Heat transfer characteristics and operational visualization of two-phase loop thermosyphon. *Appl. Therm. Eng*. **2023**, *228*, 120520. https://doi.org/10.1016/j.applthermaleng.2023.120520.
28. Yang, S.; Guo, X.; Xu, H.; Tang, F.; Zhang, B.; Zhang, Y. Experimental studies on the heat transfer characteristics and instability of a loop thermosyphon with a vertical flat evaporator for IGBT heat dissipation. *Appl. Therm. Eng*. **2025**, *264*, 125524. https://doi.org/10.1016/j.applthermaleng.2025.125524.